

Józef SALWIŃSKI*, Piotr GRĄDKOWSKI*

**INFLUENCE OF VARIATION OF SELECTED
PARAMETERS ON THE RELIABILITY
OF A THRUST BEARING OF A WATER TURBINE**

**WPLYW ZMIENNOŚCI WYBRANYCH PARAMETRÓW
NA NIEZAWODNOŚĆ ŁOŻYSKA WZDŁUŻNEGO TURBINY
WODNEJ**

Key words:

thrust bearing, elastic support, reliability, parameters randomness

Słowa kluczowe:

łożysko wzdłużne, podparcie sprężyste, niezawodność, losowość parametrów

Summary

Slide thrust bearings are composed of tilting pads. Some bearing pads are rested on sets of springs. Technical parameters of these springs are random variables. The scatter of their values may lead to bearing failure.

* AGH University of Science and Technology, Department of Machine Design and Terotechnology, al. A. Mickiewicza 30, 30-059 Kraków, e-mail: gradkow@agh.edu.pl, jsalwin@agh.edu.pl.

This article presents a method for estimating the reliability of this type of bearing in a hydrostatic phase of operation, concerning the randomness of the spring parameters as well as some parameters of the oil film.

INTRODUCTION

In many water power stations, turbine thrust bearings are built of pads, which are rest on sets of helical springs. This type of support enables circumferential tilting for hydrodynamic oil wedge creation and allows radial tilting for more uniform pressure distribution. It also allows shock and vibration absorption as well as better heat dissipation [L. 1].

This solution, however, has some disadvantages. In one of the Polish water power stations, a series of bearing failures in the initial, hydrostatic phase of performance, were reported. An excessive radial tilt of some pads occurred, which resulted in a disturbance of fluid friction conditions (Fig. 1).

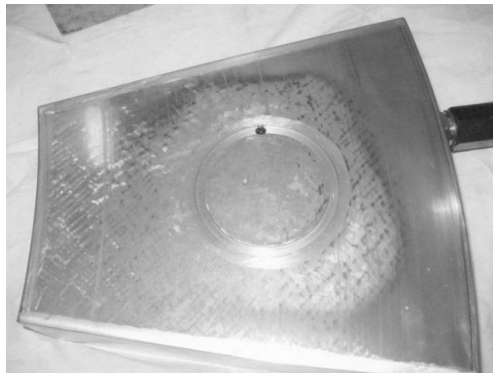


Fig. 1. Bearing pad with worn face in the external friction zone

Rys. 1. Segment z widocznymi wytarciami w strefach tarcia zewnętrznego

The analysis of the problem has led to the conclusion that one of the more important causes of the failures were the improper technical parameters of the supporting springs. Based on the spring examinations, statistical parameters, describing their length L and rate k , as well as the eccentricity of their axis of action from their geometrical axis, ρ , have been determined. These values are presented in **Table 1**.

Table 1. Basic statistical parameters of the spring sets: μ – expected value, σ – standard deviation for respective random variable

Tabela 1. Podstawowe parametry statystyczne zbiorów sprężyn: μ – wartość oczekiwana, σ – odchylenie standardowe dla odpowiedniej zmiennej losowej

Parameter		Value	Remarks
Spring length L	$\mu_L [mm]$	48,776	Cut normal distribution (a, b – limits)
	$\sigma_L [mm]$	0,0863	
	$a [mm]$	$-\infty$	
	$b [mm]$	48,9	
Spring rate k	$\mu_k [N/mm]$	4735	Normal distribution
	$\sigma_k [N/mm]$	175	
Eccentricity of the axis of action ρ	$\mu_\rho [mm]$	3,2	Uniform distribution
	$\sigma_\rho [mm]$	0,32	
	θ	$0 \dots 2\pi$	

QUALITATIVE MODEL

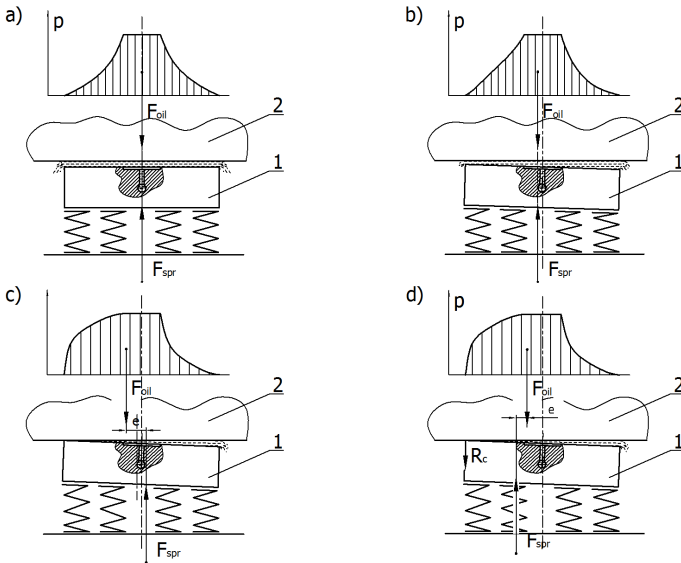


Fig. 2. System of forces acting on the bearing pad at HS lubrication phase for different parameters of supporting springs: 1 – bearing pad; 2 – slide ring; R_c – contact reaction; e – lever of the $F_{oil} - F_{spr}$ system; p – oil film pressure

Rys. 2. Układ sił działających na segment podczas smarowania hydrostatycznego dla różnych parametrów sprężyn podpierających: 1 – segment łożyska; 2 – pierścień ślizgowy; R_c – reakcja kontaktu współpracujących powierzchni; e – ramię działania pary sił $F_{oil} - F_{spr}$; p – ciśnienie filmu olejowego

The influence of the spring rate and length value scatter is illustrated in **(Fig. 2)**. If the springs are identical **(Fig. 2a)**, after switching the HS lubrication system on, the bearing pad and slide ring faces are parallel and the total oil pressure force, F_{oil} , and the resultant spring support force, F_{spr} , are balanced. If the springs' parameters are slightly scattered, the resultant spring support force will be displaced, and the pad tilted **(Fig. 2b)**. This will cause a change of the geometry of the oil film, and in consequence, a change of the pressure distribution. As a result, the pressure force will be displaced as well, and both forces will still act collinearly, keeping the pad in balance. Assuming properly selected springs, if for some reason the pad is maximally tilted (for example under some external force), the F_{oil} point of application will displace towards the narrower part of the oil film, while the point of application of F_{spr} will move towards the more compressed springs, that is in the direction opposite to F_{oil} – **Fig. 2c**. In such a case, these forces will create a moment that will tend to restore the proper position of the pad once the external force is removed. In other words, the properly selected springs should ensure stable equilibrium of the pad. However, if the spring parameters are too scattered, there is a possibility, that the two forces, F_{oil} and F_{spr} will never be able to act collinearly, no matter how deep the pad tilt is – **Fig. 2d**. In this case, after engaging the HS lubrication system, it will be impossible to generate an oil film on the entire mating surface, and a mechanical contact reaction, R_c , will appear in the system [**L. 2, 3**], and a local loss of fluid friction will occur.

Since the spring parameters, as well as the bearing load, oil viscosity and many other parameters that influence the bearing performance are random variables, determining the probability that, on any bearing pad, fluid friction conditions will be disturbed may give a valuable information for the bearing design or modernisation process. Such event may be treated as a state of failure, and its probability may be considered as the bearing reliability index.

Water turbines are not built in large series; therefore, it is hardly possible to obtain experimental data to determine their reliability. However, composing an appropriate mathematical model and subjecting it to a series of virtual experiments may allow one to determine the reliability index of a designed bearing system before its fabrication. To get reliable information, the number of the virtual experiments should be large (for example 10^4).

COMPUTATIONAL MODEL ASSUMPTIONS

Nowadays, oil film modelling is quite developed and utilises various computational methods. However, to complete the computations of more complex models, it requires several hours [L. 4]. Repeating such calculations tens of thousands of times would require amounts of time and computer resources exceeding practical implementation. Thus, some simplified approach is required.

As presented above, if the F_{oil} force is applied closer to the pad's edge than the F_{spr} , their moment will tend to restore proper position of the pad. Hence, it is enough to verify the mutual alignment of the two forces in case of maximal pad tilt. In order to quicken the calculations, an isothermal oil film model has been assumed. Experiments [L. 5] have proven that, in the hydrostatic phase of lubrication, such a model describes the pressure distribution with satisfying accuracy. Since the described failures took place in the hydrostatic phase of lubrication, the rotational speed of the turbine was assumed to be zero. Moreover, the mating faces were assumed rigid, which allowed defining the oil film thickness using the plane equation.

OIL FILM CALCULATIONS

The parameters of the oil film were determined for maximal allowable pad tilts in the direction ("azimuth") $\varphi = 0^\circ, 1^\circ, 360^\circ$ (Fig. 3). The minimum allowable oil film thickness was assumed $h_{lim} = 36 \mu m$. Pressure distribution was computed using FEM, which was incorporated in the Sequential Quadratic Programming procedure to determine the h_0 (Fig. 3) and p_0 (oil pressure in the oil groove). The whole modelling was undertaken in a MatLab environment.

The calculations were performed for three different values of load, oil viscosity, and oil flux from the oil groove, ranging $\pm 20\%$ – Table 2. These values were concatenated by a W index, defined as follows:

$$W = \frac{G \cdot B}{\eta \cdot Q} \cdot 10^{-10} \quad (1)$$

where: B – bearing pad width m[mm] (difference between the outer and inner bearing radius).

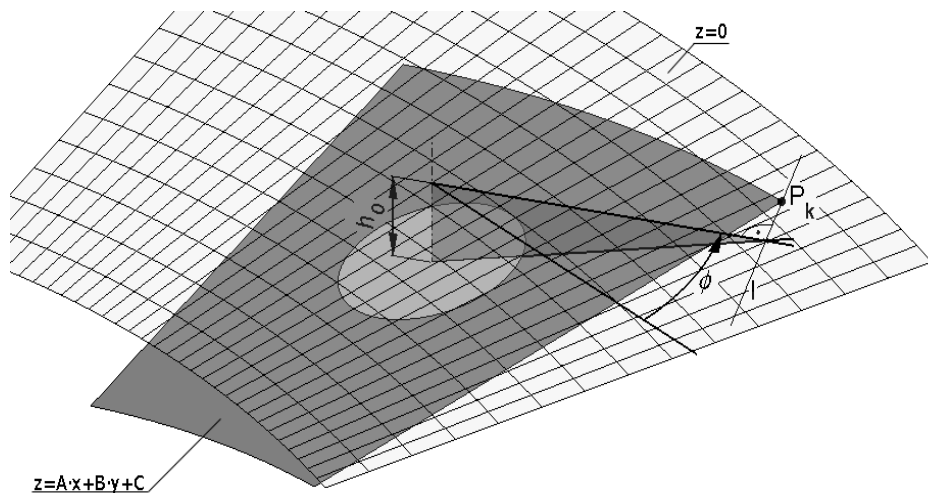


Fig. 3. Geometrical relations in case of extreme allowable pad tilt. $z = A \cdot x + B \cdot y + C$ – bearing pad face; $z = 0$ – slide ring face, ϕ – direction of the bearing pad plane inclination; P_k – point of occurrence of minimum oil film thickness, h_{lim} ; l – common line of both (slide ring and bearing pad) planes; h_0 – oil film thickness in the centre of the oil groove

Rys. 3. Ilustracja zależności geometrycznych w przypadku skrajnego dopuszczalnego pochylenia segmentu. $z = A \cdot x + B \cdot y + C$ – powierzchnia segmentu; $z = 0$ – powierzchnia pierścienia ślizgowego; ϕ – kierunek nachylenia płaszczyzny segmentu; P_k – punkt wystąpienia minimalnej grubości filmu olejowego h_{lim} ; l – prosta na przecięciu obydwu płaszczyzn; h_0 – grubość filmu olejowego w środku komory smarowej

From 27 combinations of the values presented in **Table 2**, a set of 12 unique W values was obtained. Determining the oil film parameters for each of the 27 combinations, and for 360 different ϕ values, allowed the computation of the coordinates of points of F_{oil} force application at extreme pad tilts. These points, connected with lines are shown in **Fig. 4**. They define Ω_{oil} zones limits. Ω_{oil} are zones, within which the point of application of F_{oil} force may occur.

It has been determined that the range of Ω_{oil} depends strictly on the W value. This dependency was also observed for all other parameters of the oil film. For further modelling, it was particularly important to record the values of A and B coefficients of pad plane inclination (**Fig. 3**) at different W and ϕ values.

Table 2. Constants assumed for calculations

Tabela 2. Stałe wielkości przyjęte do obliczeń

Constant		Assumed values		
		0,8x	1,0x	1,2x
Pad load	$G[N]$	107500	134375*	161250
Oil feed	$\dot{Q}[\frac{mm^2}{s}]$	42666.67	53333.33**	64000
Oil viscosity	$\eta[MPa \cdot s]$	$2.79 \cdot 10^{-8}$	$3.496 \cdot 10^{-8}$ ***	$4.19 \cdot 10^{-8}$
* – 1/16 of the entire turbine set weight, which is 215 tons ** – $3.2 dm^3/min$, capacity of the HS pump installed on the research rig [L. 5] *** – 46 cSt at density $760 kg/m^3$				

ANALYSES OF THE STOCHASTIC MODEL OF SPRING SUPPORT

Using a Monte Carlo method, the following pseudo-random parameters were generated: length, L , spring rate, k , and the eccentricity of axis of action from the spring's geometrical axis, ρ for 10000 virtual sets, 16 springs each. Spring deflections, ΔL , were calculated from systems of linear equations, where the coefficient matrix is dependent on A and B values.

For every generated set of springs, coordinates of the points of the application of F_{spr} force were calculated at three values of load (**Table 2**), and at A and B values recorded for different W values for extreme pad tilts, as well as for $A, B = 0$. The points determined in this way delimited Ω_{spr} zones, within which point of application of F_{spr} force may be expected. Based on the mutual alignment of the Ω_{spr} and the Ω_{oil} zone at given W value, the spring sets were classified either as conducive or aversive to maintaining the state of the ability of the bearing pad. **Fig. 4** presents the points of application of F_{spr} forces for each set of springs at $A, B = 0$ and at load $G = 134$ kN. Moreover, exemplary Ω_{spr} zones have been presented.

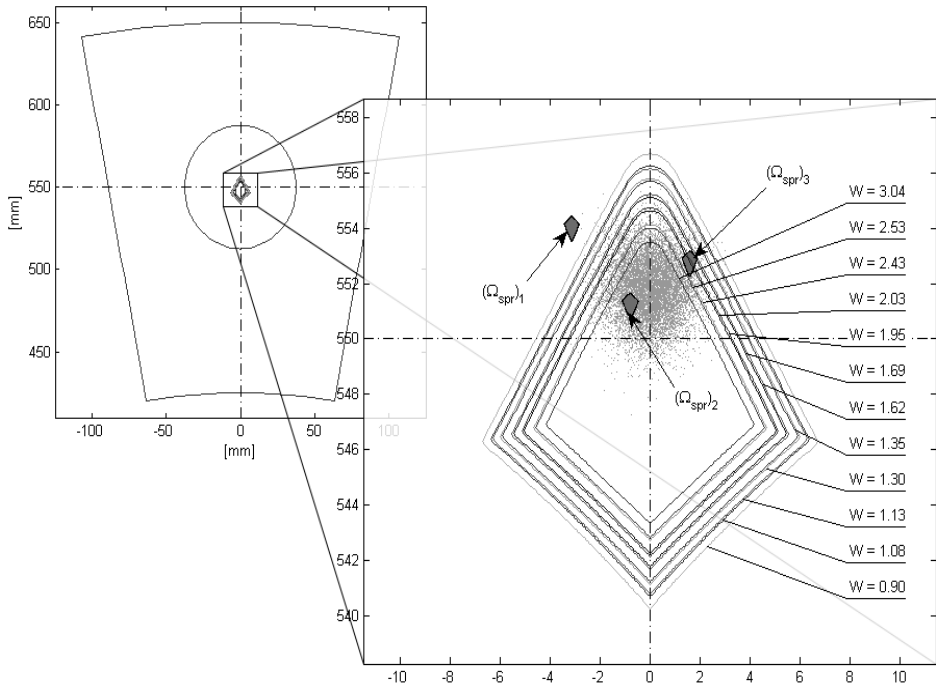


Fig. 4. The Ω_{oil} zones of possible point of application of the pressure force F_{oil} at different W index values compared to the points of application of spring support resultant forces F_{spr} at $A, B = 0$. Additional examples of Ω_{spr} zones of a possible application point of the spring support resultant force are presented

Rys. 4. Porównanie obszarów Ω_{oil} działania siły naporu przy różnych wartościach wskaźnika W z punktami przyłożenia siły F_{spr} przy $A, B = 0$, oraz przykładowe obszary Ω_{spr}

RESULTS

In **Fig. 5**, percentages of the conductive spring set cases at different W values are presented. These percentages may be considered reliability indexes for a single pad, or for a set of 16 pads, if the bearing is to be considered a serial structure, where failure of either of the pads leads to the failure of the entire structure.

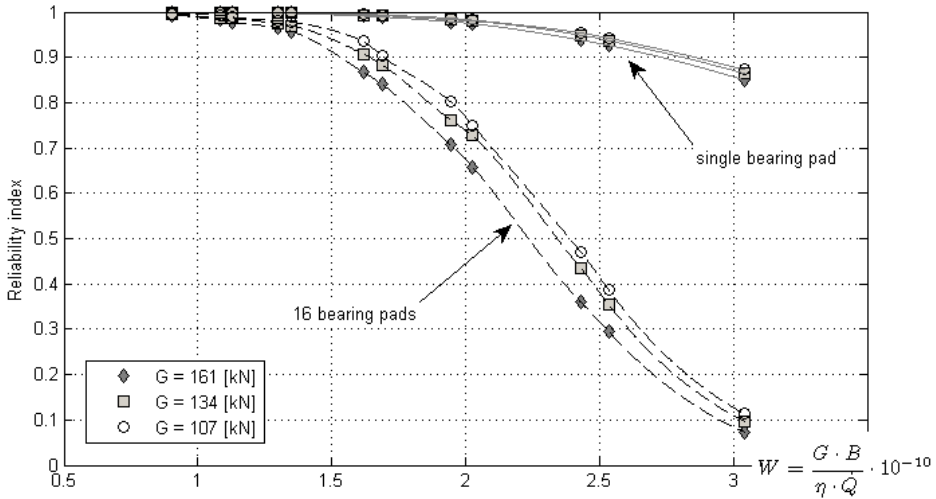


Fig. 5. Probability maintaining the state of ability of a single bearing pad and a set of 16 pads at different W index values. Curves obtained using piecewise cubic Hermite interpolation

Rys. 5. Prawdopodobieństwo pozostawania w stanie zdadności w zależności od wartości wskaźnika W dla pojedynczego segmentu, oraz dla zespołu łożyskowego złożonego z 16 segmentów. Krzywe, łączące ustalone na drodze symulacji punkty interpolowano wielomianami Hermite’a 3 stopnia

RECAPITULATION

In this article, an *a priori* method for determining a reliability index of a water turbine thrust bearing, considering the randomness of the supporting spring parameters, was presented. A dependency of this reliability index on the previously defined W index was presented.

It is interesting that the change of the oil film parameters depends on the product of the bearing load, oil viscosity and oil feed (or their inverted values), rather than on these values separately. To determine the influence of the randomness of these parameters on the bearing reliability, it is enough to determine the probability density of the W index, $f(W)$. This reduces the number of random variables in the model and allows relatively easy determination of the overall reliability index, R_a :

$$R_a = \int_{w_1}^{w_2} R(W) \cdot f(W) dW \tag{2}$$

The assumed isothermal model of the oil film is quite simple, as compared to currently used ones, e.g. the adiabatic or elastodiathermal models. However, multiple repetition of calculations forced the simplification of the model. Even so, it required more than 23 hours to determine the parameters of the oil film for each of the φ angles and 27 combinations of parameters from **Table 2**, and the very classification of spring sets at each W took more than three days.

BIBLIOGRAPHY

1. Wang X., Zhang Z., Zhang G.: The Analysis of Performance on Spring-Supported Thrust Pads Inclusive of One-Dimensional Pressure Build-up. *Journal of Shanghai University*. 1999, Vol. 3, 3, pp. 234–237.
2. Salwiński J., Rupeta W., Grądkowski P.: Nektorye aspekty modernizacji karmana v segmentnom gidrostaticheskom podpisnike gidrogeneratora. Międzynarodowa konferencja „Problemy sovermennoj mechaniki”, 2006.
3. Salwiński J., Grądkowski P.: Komputerowe modelowanie stanu równowagi segmentu łożyska wzdłużnego wspartego na zespole elementów sprężystych. *Mechanik* 2010, 1, s. 69–77, suplement.
4. Rotta G., Wasilczuk M.: Obliczeniowa analiza wybranych systemów dostarczania smaru w hydrodynamicznych łożyskach wzdłużnych. *Tribologia* 2009, 5, s. 161–169.
5. Salwiński J., Grądkowski P.: Experimental verification of a model of loss of fluid friction in a hybrid thrust bearing. *Tribologia* 2010, 3, pp. 199–208.

Recenzent:
Karol NADOLNY

Streszczenie

Ślizgowe łożyska wzdłużne zbudowane są z wahliwie umocowanych segmentów. Jednym z rozwiązań jest posadowienie segmentów na zespołach sprężyn. Parametry techniczne sprężyn są zmiennymi losowymi. Zmienność ich wartości może prowadzić do awarii zespołu łożyskowego.

W pracy przedstawiono metodę szacowania wskaźnika niezawodności łożyska w hydrostatycznej fazie pracy z uwzględnieniem losowości parametrów sprężyn, a także zmienności wybranych parametrów filmu olejowego.